

Modifying Surface Fluctuations of Polymer Melt Films with Substrate Modification

Yang Zhou,[†] Qiming He,[†] Fan Zhang,[†] Feipeng Yang,[†] Suresh Narayanan,[‡] Guangcui Yuan,[§] Ali Dhinojwala,[†] and Mark D. Foster^{*,†}

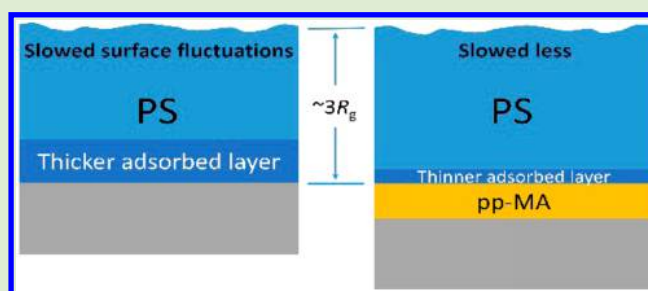
[†]Department of Polymer Science, The University of Akron, Akron, Ohio 44325, United States

[‡]X-ray Science Division, Argonne National Laboratory, Argonne, Illinois 60439, United States

[§]Center for Neutron Research, National Institute of Standards and Technology, Gaithersburg, Maryland 20899, United States

Supporting Information

ABSTRACT: Deposition of a plasma polymerized film on a silicon substrate substantially changes the fluctuations on the surface of a sufficiently thin melt polystyrene (PS) film atop the substrate. Surface fluctuation relaxation times measured with X-ray photon correlation spectroscopy (XPCS) for ca. $4R_g$ thick melt films of 131 kg/mol linear PS on hydrogen-passivated silicon (H-Si) and on a plasma polymer modified silicon wafer can both be described using a hydrodynamic continuum theory (HCT) that assumes the film is characterized throughout its depth by the bulk viscosity. However, when the film thickness is reduced to $\sim 3R_g$, confinement effects are evident. The surface fluctuations are slower than predicted using the HCT, and the confinement effect for the PS on H-Si is larger than that for the PS on the plasma polymerized film. This deviation is due to a difference in the thicknesses of the strongly adsorbed layers at the substrate which are impacted by the substrate surface energy.



Surface fluctuations on polymer melts play important roles in determining wetting, adhesion,¹ and tribology. The surface fluctuations depend not only on the movement of polymer chains at the surface but also on movement of chains deeper in the film.² Recent developments in XPCS have made it possible to probe the surface fluctuations at temperatures much higher than $T_{g,bulk}$.^{2–12} Kim et al.² found that the surface relaxation times, τ , of entangled linear polystyrene (PS) melt films can be described well with a HCT theory.¹³ HCT predicts a universal curve for films with different thicknesses, h , when the data are plotted as normalized relaxation time, τ/h , as a function of dimensionless in-plane scattering vector, $q_{||}h$.

Surface fluctuations of sufficiently thin polymer films manifest confinement effects. Wang et al.¹⁴ probed confinement with surface fluctuations for films of 90 kg/mol PS by static diffuse X-ray scattering. They attributed the suppression of surface fluctuations to van der Waals interactions between the melt surface and underlying substrate. Jiang and coauthors¹⁰ conjectured that physisorption of chain segments to the substrate could restrict chain motion, resulting in an elastic component to the viscoelastic behavior in films of entangled chains having thicknesses equal to only a few times R_g . The surface fluctuations of a small cyclic PS melt film^{5,9} evidence confinement effects already at a film thickness of $14R_g$. In comparison, films of the linear analogue polymer do not manifest confinement effects even at a thickness of $7R_g$. The different thicknesses for the onset of confinement effects were attributed to the different thicknesses of strongly adsorbed

layers at the substrate for the two chain architectures, cyclic and linear.

Recently, several research groups^{9,15–22} have utilized the approach proposed by Guiselin²³ to characterize the formation and structure of strongly adsorbed layers. Fuji et al.¹⁵ and Gin et al.¹⁷ showed that the thickness of a strongly adsorbed layer of linear chains increases with molecular weight and annealing time. They argued based on the observed differences in the behavior for films on H-Si and silica substrates (silicon wafers with native oxide layer) that the surface energy of the substrate plays a role as well. The thickness of the strongly adsorbed layer in a film annealed for a long time on a H-Si substrate is $0.34R_g$ higher than it is on a silica substrate.¹⁵ There is growing evidence^{3,16,24,25} that the adsorbed layer at the substrate interface affects various properties of supported polymer thin films via long-range perturbations. Thus, it should be possible to modify the film properties by modifying the substrate to change the character of the strongly adsorbed layer. In this letter, we demonstrate that a film's surface fluctuations can be readily impacted by tailoring the substrate surface energy with a very thin plasma polymerized coating that does not significantly interpenetrate the film. This suggests a route for changing the

Received: June 24, 2017

Accepted: August 4, 2017

Published: August 14, 2017

film surface wetting and adhesion properties by just changing the substrate.

Surface fluctuations of PS on H–Si and plasma polymerized maleic anhydride (ppMA) coated silicon wafers were investigated with XPCS. According to the HCT theory, the surface of a viscous fluid film should exhibit overdamped capillary waves with a relaxation time that depends on film viscosity, surface tension, film thickness, and wave vector.^{2,13}

When a nonslip boundary condition holds at the film–substrate interface, the thickness normalized relaxation time is given as a function of $q_{\parallel}h$ as

$$\frac{\tau}{h} = \frac{2\eta[\cosh^2(q_{\parallel}h) + (q_{\parallel}h)^2]}{\gamma q_{\parallel}h[\cosh(q_{\parallel}h)\sinh(q_{\parallel}h) - q_{\parallel}h]} \quad (1)$$

Surface tension and bulk viscosity values for 131 kg/mol linear PS at different temperatures, listed in Table 1, were interpolated from literature data.^{26,27}

Table 1. Surface Tensions and Bulk Viscosities of 131 kg/mol Linear PS at Various Temperatures

temp (°C)	γ_{linear}^a (mN/m)	η_{bulk} (Pa s)
150	31.3	3.4×10^6
160	30.6	9.7×10^5
170	29.9	3.1×10^5
180	29.3	1.2×10^5

^aThe uncertainty in the surface tension is about $\pm 5\%$.

There is no difference in the normalized relaxation times for PS films on H–Si and ppMA when the films are of thickness about $4R_g$ (R_g is 9.85 nm for 131 kg/mol PS). Normalized relaxation times for a 40.7 ± 0.1 nm thick film of PS on H–Si and a 44.1 ± 0.1 nm thick PS film on ppMA are shown in Figure 1. The data collapse onto a universal curve for each

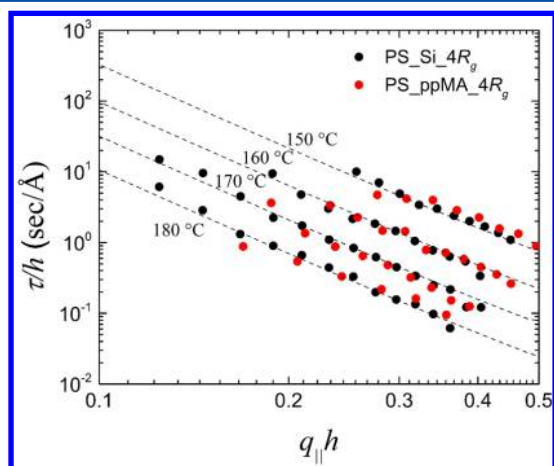


Figure 1. τ/h vs $q_{\parallel}h$ for PS on H–Si substrate and ppMA film. The dashed curves are calculated based on the HCT theory with corresponding γ_{linear} and η_{bulk} .

temperature, and no confinement is observed. However, for films of about $3R_g$ thickness (34.5 ± 0.1 nm on H–Si, 33.0 ± 0.1 nm on ppMA), the normalized relaxation times do not collapse onto the universal curves and the discrepancy is larger for the H–Si substrate, as shown in Figure 2. For both 170 and 180 °C, τ/h for the $3R_g$ film on H–Si is about five times larger

than the universal curve value. On ppMA, it is only two times larger.

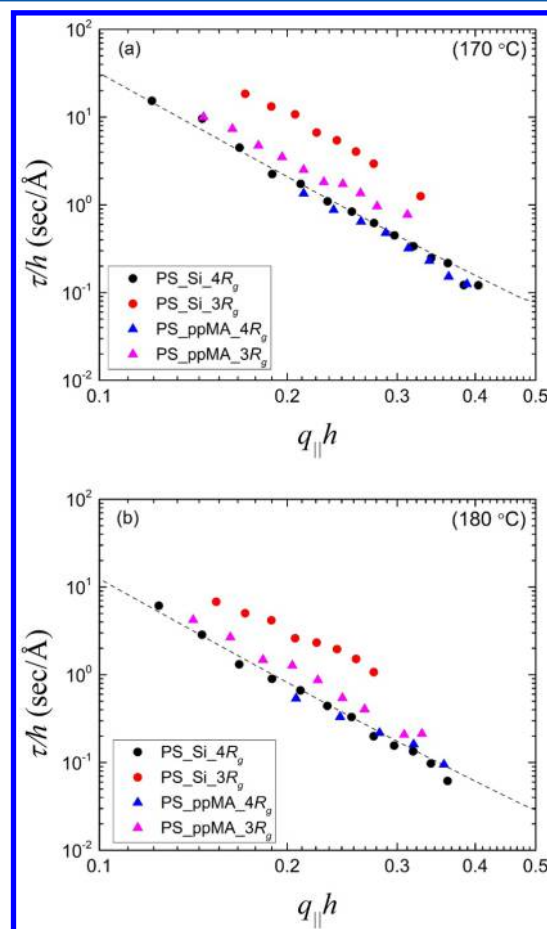


Figure 2. τ/h vs $q_{\parallel}h$ for PS thin films with thicknesses about $4R_g$ and $3R_g$ on a H–Si substrate and ppMA coating at (a) 170 °C and (b) 180 °C. The dashed curves are calculated with the HCT using the bulk viscosity, η_{bulk} .

The difference in confinement on the two substrates is not due to differences in the modulus of the substrate or to differences in interpenetration with the substrate. Torkelson and co-workers⁴ found that τ of a PS film tracks with the modulus of a 500–700 nm thick layer underneath the PS film when the temperature is slightly above T_g . Here, however, the plasma polymerized coating deposited on silicon is only about 10 nm thick. Thus, the effective modulus of the ppMA coated substrate should be close to that of the bare H–Si wafer, so a modulus difference is not the cause for difference in confinement. Uğur et al.²⁸ found that the surface fluctuations of a layer of untethered PS chains were slowed when that layer interpenetrated with an underlying brush. Here the neutron scattering length density (NSLD) profiles obtained from neutron reflectivity (NR) for the interfaces between deuterated PS (dPS) and the two types of substrate are quite similar and both are sharp. The interfacial profile for a 20 nm thick 144 kg/mol dPS film atop a ppMA coating (see Supporting Information (SI), Figure S1) is represented well by an error function with $\sigma = 4$ Å. This is consistent with values of interface width seen previously for PS on Si.²⁹

We propose that the difference in confinement seen for these two substrate surfaces is due to differences in the structure of a

strongly adsorbed layer at the substrate interface. It is possible to rationalize the data for the PS films of $\sim 3R_g$ thickness by simply postulating that the film on H–Si has a uniform viscosity five times the bulk value and that the film on ppMA has a uniform viscosity two times the bulk value. However, there is evidence that a model with at least two layers of different viscosities better represents the structure behind the dynamics.^{9,30}

XR measurements can reveal the presence of a irreversibly adsorbed layer remaining on a substrate after rinsing.^{15,17,31} This is a collapsed version of the layer present in the melt of most strongly adsorbed chains, containing trains, loops, and tails.³² After annealing, the irreversibly adsorbed layer seen on Si after rinsing with toluene is ~ 5 nm ($\sim 0.5R_g$) thick, consistent with thicknesses seen by other researchers^{15,17,18,33} for similar molecular weight, annealing time, and temperature. Strikingly, no irreversibly adsorbed layer is seen on the ppMA coating. The ppMA coating is highly cross-linked and adheres well to the silicon substrate even after soaking in toluene. Thus, the absence of an irreversibly adsorbed layer is not due to damage of the plasma polymerized coating. Rather, it reflects a strong difference in the adsorbed layer that is present in the melt film at the temperature at which the surface fluctuations were measured.

As a first approximation, we can assume that the structure in the melt film during XPCS measurement may be represented with two layers, one at the substrate that has extremely high viscosity (assume $\eta \rightarrow \infty$) and a second of bulk viscosity next to air. Then the appropriate thickness must be assigned to the adsorbed layer assumed to have extremely high viscosity. He et al.⁹ were able to rationalize the data from melt films of 6 kg/mol cyclic PS chains using such a model. At 140 °C, this model worked for several confined films if the extremely high viscosity layer thickness was set equal to the thickness of the irreversibly adsorbed layer. However, the thickness assumed for the extremely viscous layer in the melt had to be increased significantly to rationalize data at two higher temperatures. The agreement between irreversibly adsorbed layer thickness and thickness of the extremely viscous layer at one temperature appears to have been fortuitous. Here, using an extremely viscous layer thickness equal to the irreversibly adsorbed layer thickness for the $3R_g$ PS film on Si does not provide agreement with the universal curve (see SI, Figure S2). However, if we allow the thickness of the extremely viscous layer to vary as a fitting parameter, we can self-consistently fit the data for both substrates and both overall film thicknesses at both temperatures. The 170 °C data from both the $3R_g$ and $4R_g$ thick films collapse together using the two-layer model with a 27 nm extremely viscous layer on H–Si and a 15 nm extremely viscous layer on ppMA, as shown in Figure 3. We recognize that the two layer model using an extremely viscous layer is an approximation. Most probably, the actual structure involves a more moderate gradient in viscosity between the “extremely viscous” and “bulk viscosity” regions.

Nonetheless, what consideration of this simple model makes clear is that whatever the substrate influence on the melt, this influence must extend over a distance from the substrate considerably larger than the thickness of the irreversibly adsorbed layer present after rinsing. This suggestion is consistent with the finding of Koga et al.³ that in a 57 nm thick annealed melt film of 123 kg/mol PS on H–Si, the viscosity in a region around 30 nm (or $\sim 3R_g$) above the substrate is a factor of 10 above that of the bulk. In a 32 nm

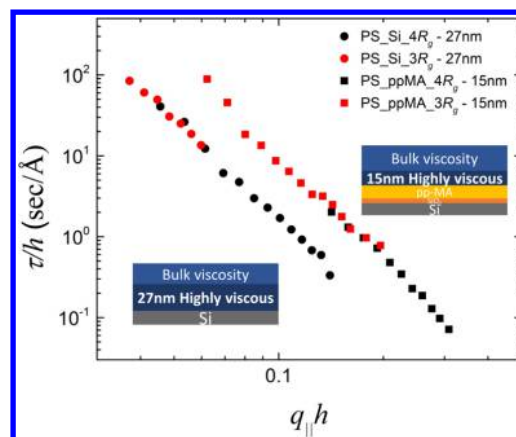


Figure 3. τ/h vs $q_{\parallel}h$ at 170 °C for PS thin films on H–Si and ppMA assuming effective thicknesses reflecting reductions from the actual thicknesses by the amounts shown in the legend.

thick film, they find the enhancement in viscosity in the film center to be even more dramatic. In their picture, the entanglement of polymers with the network of the adsorbed layer propagates the mobility reduction of the irreversibly adsorbed layer over distances larger than the coil size. Simulations³² show that the adsorbed layer contains polymer chains with tails that are nonuniformly stretched and that these tails extend farther up into the film for stiffer chains such as PS. Those authors argue that chain conformations are perturbed up to distances of $3R_g$ from the substrate for flexible chains and even higher for stiff chains. This is consistent with our finding that the surface fluctuations are strongly perturbed by a region of very high viscosity at the substrate for films of thickness $3R_g$.

In the melt state, there is a layer of adsorbed chains on both the Si and ppMA substrates, but on ppMA after annealing, none of this layer is bound tightly enough to withstand rinsing with toluene. This is because the PS segment–substrate interactions and PS chain conformations next to the substrate are different for the two substrates. There are both simulations and experimental findings to support this supposition. Richter et al.³⁴ found experimentally that the molecular orientation of phenyl groups of PS next to a substrate varied as the substrate surface was changed from hydrophobic to hydrophilic. They correlated this different interface structure of PS with the adhesion of PS to hydrophobic and hydrophilic substrates. Tsige and co-workers³⁵ found with molecular dynamics simulations that the density and structural properties of the phenyl rings depend on the type of substrate (quartz, silica, or graphite). In our case, the water contact angle of the ppMA coating is $42^\circ \pm 2$, while that of H–Si is around 70° .³⁶ We propose that the conformations of the PS chains are different at these two different substrate surfaces, leading to strong differences in confinement. Our future work will focus on characterizing with sum frequency generation spectroscopy^{37,38} the polymer chain conformation next to the plasma polymerized coating.

EXPERIMENTAL SECTION

Films of linear PS ($M_w = 131000$ g/mol; PDI = 1.02; synthesized by anionic polymerization) were spun-cast from toluene (EMD, 99.5%) solutions onto clean³⁹ silicon wafers from which the native oxide has been etched and onto unetched silicon wafers coated using plasma polymerization. The plasma polymerized coatings were deposited from maleic anhydride monomer (Sigma-Aldrich) in a custom-built,

inductively coupled, and rf-driven ($f = 13.56$ MHz) reactor.⁴⁰ All films were annealed in high vacuum (ca. 1×10^{-7} Pa) at 150 °C for 15 h before the XPCS measurements. The interface width between a film of deuterated PS ($M_w = 144000$ g/mol; PDI = 1.13; Polymer Source) and the ppMA coating was quantified with NR performed at the National Institute of Standards and Technology NG-7 horizontal reflectometer ($\lambda = 0.475$ nm).

XPCS experiments were performed at beamline 8-IDI at the Advanced Photon Source using a previously described geometry and analysis procedure.^{2,5} A coherent X-ray beam (7.35 keV, $20 \times 20 \mu\text{m}^2$) probed the film surface with an incident angle of 0.14°, below the critical angle of PS (0.16°). The intensity was recorded using a two-dimensional CCD camera after equilibrating a sample for 20 min at a given temperature. Fluctuations in the off-specular scattering were analyzed to yield the intensity autocorrelation function, g_2 , given by

$$g_2(q_{\parallel}, t) = \frac{\langle I(q_{\parallel}, t')I(q_{\parallel}, t' + t) \rangle}{\langle I(q_{\parallel}, t') \rangle^2} \quad (2)$$

where $I(q_{\parallel}, t')$ is the scattering intensity at wave vector transfer q_{\parallel} at time t' , and the angular brackets refer to ensemble averages for the delay time, t . The correlation functions were fit well by a single-exponential decay, $g_2 = 1 + \beta \exp(-2t/\tau)$, with β being the coherent contrast and τ being the relaxation time.

■ ASSOCIATED CONTENT

Supporting Information

The Supporting Information is available free of charge on the ACS Publications website at DOI: 10.1021/acsmacrolett.7b00459.

Neutron reflectivity of dPS on ppMA and XPCS results of PS on two substrates with normalized thickness equal to the full thickness minus the irreversibly adsorbed layer thickness (PDF)

■ AUTHOR INFORMATION

Corresponding Author

*E-mail: mdf1@uakron.edu.

ORCID

Yang Zhou: 0000-0002-4276-6253

Ali Dhinojwala: 0000-0002-3935-7467

Mark D. Foster: 0000-0002-9201-5183

Notes

The authors declare no competing financial interest.

■ ACKNOWLEDGMENTS

This work was supported by funding from DoD through the TCC (FA7000-14-2-20016) and DURIP (W911NF-09-1-0122). Use of the Advanced Photon Source at Argonne National Laboratory was supported by the DOE's Office of Science under contract DE-AC02-06-CH11357. We acknowledge support of the National Institute of Standards and Technology, U.S. Department of Commerce, in providing the neutron research facilities used in this work. The identification of commercial products does not imply endorsement by the National Institute of Standards and Technology nor does it imply that these are the best for the purpose.

■ REFERENCES

- (1) Tang, T.; Jagota, A.; Hui, C. Y.; Chaudhury, M. J. *Adhes.* **2006**, *82*, 671.
- (2) Kim, H.; Rühm, A.; Lurio, L. B.; Basu, J. K.; Lal, J.; Lumma, D.; Mochrie, S. G. J.; Sinha, S. K. *Phys. Rev. Lett.* **2003**, *90*, 68302.
- (3) Koga, T.; Jiang, N.; Gin, P.; Endoh, M. K.; Narayanan, S.; Lurio, L. B.; Sinha, S. K. *Phys. Rev. Lett.* **2011**, *107*, 225901.
- (4) Evans, C. M.; Narayanan, S.; Jiang, Z.; Torkelson, J. M. *Phys. Rev. Lett.* **2012**, *109*, 38302.
- (5) Wang, S. F.; Jiang, Z.; Narayanan, S.; Foster, M. D. *Macromolecules* **2012**, *45*, 6210–6219.
- (6) Wang, S. F.; Yang, S.; Lee, J.; Akgun, B.; Wu, D. T.; Foster, M. D. *Phys. Rev. Lett.* **2013**, *111*, 68303.
- (7) Liu, B.; Narayanan, S.; Wu, D. T.; Foster, M. D. *Macromolecules* **2013**, *46*, 3190–3197.
- (8) Sinha, S. K.; Jiang, Z.; Lurio, L. B. *Adv. Mater.* **2014**, *26*, 7764–7785.
- (9) He, Q.; Narayanan, S.; Wu, D. T.; Foster, M. D. *ACS Macro Lett.* **2016**, *5*, 999–1003.
- (10) Jiang, Z.; Kim, H.; Jiao, X.; Lee, H.; Lee, Y. J.; Byun, Y.; Song, S.; Eom, D.; Li, C.; Rafailovich, M. H.; Lurio, L. B.; Sinha, S. K. *Phys. Rev. Lett.* **2007**, *98*, 227801.
- (11) Jiang, Z.; Mukhopadhyay, M. K.; Song, S.; Narayanan, S.; Lurio, L. B.; Kim, H.; Sinha, S. K. *Phys. Rev. Lett.* **2008**, *101*, 246104.
- (12) Mukhopadhyay, M. K.; Jiao, X.; Lurio, L. B.; Jiang, Z.; Stark, J.; Sprung, M.; Narayanan, S.; Sandy, A. R.; Sinha, S. K. *Phys. Rev. Lett.* **2008**, *101*, 115501.
- (13) Jackle, J. J. *J. Phys.: Condens. Matter* **1998**, *10*, 7121–7131.
- (14) Wang, J.; Tolan, M.; Seock, O. H.; Sinha, S. K.; Bahr, O.; Rafailovich, M.; Sokolov, J. C. C. *Phys. Rev. Lett.* **1999**, *83*, 564–567.
- (15) Fujii, Y.; Yang, Z.; Leach, J.; Atarashi, H.; Tanaka, K.; Tsui, O. K. C. *Macromolecules* **2009**, *42*, 7418–7422.
- (16) Napolitano, S.; Wübbenhorst, M. *Nat. Commun.* **2011**, *2*, 260.
- (17) Gin, P.; Jiang, N.; Liang, C.; Taniguchi, T.; Akgun, B.; Satija, S. K.; Endoh, M. K.; Koga, T. *Phys. Rev. Lett.* **2012**, *109*, 265501.
- (18) Jiang, N.; Shang, J.; Di, X.; Endoh, M. K.; Koga, T. *Macromolecules* **2014**, *47*, 2682–2689.
- (19) Jiang, N.; Wang, J.; Di, X.; Cheung, J.; Zeng, W.; Endoh, M. K.; Koga, T.; Satija, S. K. *Soft Matter* **2016**, *12*, 1801–1809.
- (20) Bal, J. K.; Beuvier, T.; Unni, A. B.; Chavez Panduro, E. A.; Vignaud, G.; Delorme, N.; Chebil, M. S.; Grohens, Y.; Gibaud, A. *ACS Nano* **2015**, *9*, 8184–8193.
- (21) Beena Unni, A.; Vignaud, G.; Bal, J. K.; Delorme, N.; Beuvier, T.; Thomas, S.; Grohens, Y.; Gibaud, A. *Macromolecules* **2016**, *49*, 1807–1815.
- (22) Burroughs, M. J.; Napolitano, S.; Cangialosi, D.; Priestley, R. D. *Macromolecules* **2016**, *49*, 4647–4655.
- (23) Guiselin, O. *Europhys. Lett.* **1992**, *17*, 225–230.
- (24) Napolitano, S.; Glynos, E.; Tito, N. B. *Rep. Prog. Phys.* **2017**, *80*, 036602.
- (25) Napolitano, S.; Sferrazza, M. *Adv. Colloid Interface Sci.* **2017**, DOI: 10.1016/j.cis.2017.02.003.
- (26) Pu, Z. *Polymer Data Handbook*; 2nd ed.; Oxford University Press: New York, 2009.
- (27) Plazek, D. J.; O'Rourke, V. M. *Polym. Sci. Part A-2* **1971**, *9*, 209–243.
- (28) Uğur, G.; Akgun, B.; Jiang, Z.; Narayanan, S.; Satija, S.; Foster, M. D. *Soft Matter* **2016**, *12*, 5372–5377.
- (29) Russell, T. P. *Mater. Sci. Rep.* **1990**, *5*, 171–271.
- (30) Li, R. N.; Chen, F.; Lam, C. H.; Tsui, O. K. C. *Macromolecules* **2013**, *46* (19), 7889–7893.
- (31) Braatz, M. L.; Infantas Melendez, L.; Sferrazza, M.; Napolitano, S. *J. Chem. Phys.* **2017**, *146*, 203304.
- (32) Carrillo, J. M. Y.; Cheng, S.; Kumar, R.; Goswami, M.; Sokolov, A. P.; Sumpter, B. G. *Macromolecules* **2015**, *48*, 4207–4219.
- (33) Housmans, C.; Sferrazza, M.; Napolitano, S. *Macromolecules* **2014**, *47*, 3390–3393.
- (34) Wilson, P. T.; Richter, L. J.; Wallace, W. E.; Briggman, K. A.; Stephenson, J. C. *Chem. Phys. Lett.* **2002**, *363*, 161–168.
- (35) Tatek, Y. B.; Tsige, M. J. *J. Chem. Phys.* **2011**, *135*, 174708.
- (36) Adachi, S.; Arai, T.; Kobayashi, K. J. *J. Appl. Phys.* **1996**, *80*, 5422.
- (37) Harp, G. P.; Gautam, K. S.; Dhinojwala, A. J. *J. Am. Chem. Soc.* **2002**, *124*, 7908–7909.

(38) Gautam, K. S.; Schwab, A. D.; Dhinojwala, A.; Zhang, D.; Dougal, S. M.; Yeganeh, M. S. *Phys. Rev. Lett.* **2000**, *85*, 3854–3857.

(39) Piranha solution is corrosive, so acid-resistant gloves, protective goggles, and lab coats are required when handling the piranha solution.

(40) Badge, I.; Bhawalkar, S. P.; Jia, L.; Dhinojwala, A. *Soft Matter* **2013**, *9*, 3032.